Commun Nonlinear Sci Numer Simulat 19 (2014) 3827–3844

Contents lists available at ScienceDirect

Commun Nonlinear Sci Numer Simulat

journal homepage: www.elsevier.com/locate/cnsns

Dynamics of an HIV-1 infection model with cell mediated immunity

Pei Yu [a,*], Jianing Huang [a], Jiao Jiang [b]

[a] Department of Applied Mathematics, Western University London, Ontario N6A 5B7, Canada
[b] Department of Mathematics, Shanghai Maritime University, Shanghai 201306, China

ARTICLE INFO

Article history:
Received 18 February 2014
Accepted 2 March 2014
Available online 12 March 2014

Keywords:
HIV-1 infection model
Cell mediated immunity
Lyapunov function
Routh–Hurwitz condition
Stability
Normal form theory

ABSTRACT

In this paper, we study the dynamics of an improved mathematical model on HIV-1 virus with cell mediated immunity. This new 5-dimensional model is based on the combination of a basic 3-dimensional HIV-1 model and a 4-dimensional immunity response model, which more realistically describes dynamics between the uninfected cells, infected cells, virus, the CTL response cells and CTL effector cells. Our 5-dimensional model may be reduced to the 4-dimensional model by applying a quasi-steady state assumption on the variable of virus. However, it is shown in this paper that virus is necessary to be involved in the modeling, and that a quasi-steady state assumption should be applied carefully, which may miss some important dynamical behavior of the system. Detailed bifurcation analysis is given to show that the system has three equilibrium solutions, namely the infection-free equilibrium, the infectious equilibrium without CTL, and the infectious equilibrium with CTL, and a series of bifurcations including two transcritical bifurcations and one or two possible Hopf bifurcations occur from these three equilibria as the basic reproduction number is varied. The mathematical methods applied in this paper include characteristic equations, Routh–Hurwitz condition, fluctuation lemma, Lyapunov function and computation of normal forms. Numerical simulation is also presented to demonstrate the applicability of the theoretical predictions.

© 2014 Elsevier B.V. All rights reserved.

1. Introduction

In the past a few decades, great progress on disease modeling has been achieved and many mathematical methods have been developed. Today, based on experimental works, scientists can establish more realistic models and use more advanced mathematical tools to better understand the dynamic properties of the viral infection in the level of cells. These improvements allow us to study the dynamical relationship between the host cells and the virus or even more complicated, with new cells generated by the body in order to kill virus. These models are of especial importance to human beings because they may provide useful information for medical scientists to better understand the interactions of all the components related to the infection of virus. For example, how does virus infect human beings? How does the immune system respond to the invasion of virus? Which part of the responses is the most important compared to other factors? To properly answer these questions, it requires developing more realistic models and new methodologies for analyzing the models.

* Corresponding author. Fax: +1 519 661 3523.
E-mail addresses: pyu@uwo.ca (P. Yu), jhuan233@uwo.ca (J. Huang), jiaojiang@shmtu.edu.cn (J. Jiang).

http://dx.doi.org/10.1016/j.cnsns.2014.03.002
1007-5704/© 2014 Elsevier B.V. All rights reserved.

Among the disease models, the HIV-1 models are very important since the AIDs is mainly due to HIV and is still not curable today. It should be noted that such kind of virus sometimes cannot even be detected in human body because the virus load is extremely low. A common therapy used frequently in HIV-1 case is called Highly Active Antiretroviral Therapy (HAART) [1] based on the administration of at least three different drugs from two or more classes. The viral decline in the presence of combination therapy is a significant result in curing AIDS. At first, adopting the HAART will cause the viral load to decline rapidly, which is called the first phase, and then there will be a slower phase following the first phase [2–4]. Several months after the patients adopt the therapy, the viral load will be below the level of detection, which is called the third phase [2–4]. However, this does not mean that the virus has been completely cleared. Even today's modern medical treatment could suppress a patient's virus load to a low level for many years, the low level of viremia can still be detected in many patients who have received the HAART treatment for many years. This has been observed from the transient episodes of viremia above the detection limit [2–4]. This interesting phenomenon is called infection recurrence or viral blips, which has attracted many researchers to study and a recent article has given a detailed analysis and proposed a hypothesis to explain how this phenomenon is generated [5]. The main reason for this phenomenon to happen is that the HIV-1 establishes a latent infection in resting memory $CD4^+$ T cells. In other words, the $CD4^+$ memory cells serve as a latent reservoir for HIV [6]. Even after the third phase of the therapy when the virus cannot be detected, the latent reservoir decays so slowly that the virus persist due to the presence of the latent infected $CD4^+$ cells. These $CD4^+$cells will not produce virus until they are activated and they always have a long life span. During their resting, they will not be found by the immunosurveillance T cells. So they will be latent during the drug therapy (that's why they are called latent infected cells). This kind of T cells thus becomes a serious obstacle in completely clearing the virus [7,8].

A virus cannot replicate by itself, and it must take over host cells and use them to replicate [9]. First, HIV-1 viruses attack $CD4^+$ T cells (which have $CD4^+$ receptors, sometimes called helper T-cells), and kill the $CD4^+$ T cells. Then, the viruses insert their own DNA into the DNA of the host cells and produce viral particles that can infect other healthy cells [9]. In the real situation, the immune system will respond to the viral infection [6]. The response is called cytotoxic T lymphocytes (CTLs), which are the T cells that are able to recognize and kill the cells infected by HIV-1 viruses. In general, since they lack $CD4^+$ receptor, they would not be infected by HIV-1 viruses. Once the cytotoxic T cells are activated, they will travel around the body and search for the infected cells. Once an infected cell is found, the so-called programmed cell death or apoptosis will take action to kill the infected cells. This procedure can cause the cellular nuclear blebbing and eventually, fragmentation of the DNA, and thus the cell destroys itself. So the cytotoxic T cells kill the infected cells by letting them undergo apoptosis [10,11].

From the above described procedure, the first reason for the amount of T cells to decline is due to the viruses which invade the host cells and use them to replicate, and then infect more T cells, resulting in a decline of the level of $CD4^+$ T cells. The second reason is due to the immune system, which responds to the infection and activate the cytotoxic T lymphocytes (CTLs), and then releases the killer cells to kill the infected $CD4^+$ T cells, causing the $CD4^+$ T cell to decline to a lower level. Having experienced these two stages, the amount of T cells has been reduced to a critical level and the cell-mediated immunity of the human body is lost and the body becomes extremely susceptible to possible infections. Furthermore, the CTLs response should also be responsible for the damage of the human body because in order to kill the viruses, the killer T cells will kill every cell that has been infected by the HIV-1 virus, many of which are merely tissue cells [12].

In order to study the immune response during a viral infection, many models have been developed. Among them, a model developed in [13,14], which describes more accurately the dynamics of CTL response in the immune system, has been recently studied extensively in [9]. The model is given in the form of a 4-dimensional system of differential equations as follows.

$$\begin{aligned} \dot{x} &= \lambda - dx - \beta xy, \\ \dot{y} &= \beta xy - ay - pyz, \\ \dot{w} &= cyw - cqyw - bw, \\ \dot{z} &= cqyw - hz, \end{aligned} \tag{1}$$

where a dot denotes differentiation with respect to time t, the variables x, y, w and z represent the density of the uninfected cells, the infected cells, the CTL response (CTLp) cells and CTL effector (CTLe) cells, respectively. All parameters are positive, and $0 < q < 1$, guaranteeing that $(1 - q) > 0$. Uninfected cells are produced at a constant rate λ, and die at a rate of dx, implying that the average life-time of an uninfected cell is $\frac{1}{d}$. The uninfected cells may become infected cells at a rate of βxy, and the infected cells die at a rate of ay, and removed by the CTLes at a rate of pyz. The CTL response cells emerge at a rate of cyw, and they may become effector cells at a rate of $cqyw$ or cleared away at a rate bw. Similarly, the effector cells are created at a rate of $cqyw$ and cleared away at a rate hz.

The dynamical properties of model (1) have been recently studied in detail by Chan and Yu [9]. It is shown that the system can have three equilibrium solutions and a series of bifurcations occur through these equilibrium solutions, via two transcritical bifurcations and one Hopf bifurcation. The particular interest is that this system can have Hopf bifurcation, giving rise to periodically oscillating solutions, which describe the real complex situation more accurately. If we only consider the CTLe in system (1), that is, combining the CTLps to the CTLes, and thus omitting the third equation and letting $w = z$ in the fourth equation yields the following 3-dimensional model [13,15],

$$\begin{aligned}\dot{x} &= \lambda - dx - \beta xy,\\ \dot{y} &= \beta xy - ay - pyz,\\ \dot{z} &= cyz - hz.\end{aligned} \tag{2}$$

Note in this model that the CTLes are not infected by virus because of lack of $CD4^+$ receptors. It is easy to show that model (2) also has three equilibrium solutions, but with only transcritical bifurcations through the three equilibrium solutions. This indicates that this 3-dimensional model is not able to catch the complex dynamical behavior of the real situation.

Another very basic 3-dimensional model, which is frequently used as an introductory model for the study of HIV infection, can be obtained from model (2) by removing the CLTes (the variable z) and introducing virus (the v variable) into the model, given in [15,16]:

$$\begin{aligned}\dot{x} &= \lambda - dx - \beta xv,\\ \dot{y} &= \beta xv - ay,\\ \dot{v} &= ky - uv,\end{aligned} \tag{3}$$

where v represents the density of the virus, which is replicated at a rate of ky and is cleared at a rate of uv. Reversely, we can also consider model (2) being obtained from model (3) by assuming a quasi-steady state on the virus v (i.e., $\dot{v} = 0$) and introducing the CLT response (the z variable). It is well known that the model (3) has only two equilibrium solutions: infection-free equilibrium and infected equilibrium. These two equilibria are either unstable or globally asymptotically stable, and they exchange their stability at a transcritical point. Therefore, it is not a realistic model to study dynamical behavior of immune systems.

Although the model (1) has been shown to be a good model in studying dynamical behaviors (e.g., the Hopf bifurcation), it is still not perfect since it does not contain the virus, or it has assumed a quasi-steady state on the virus. In order to more realistically model the immune system, we combine systems (3) and (1) to have the following 5-dimensional system:

$$\begin{aligned}\dot{x} &= \lambda - dx - \beta xv,\\ \dot{y} &= \beta xv - ay - pyz,\\ \dot{v} &= ky - uv,\\ \dot{w} &= cyw - cqyw - bw,\\ \dot{z} &= cqyw - hz.\end{aligned} \tag{4}$$

It has been noted that a similar 5-dimensional model was given in [17], described by (there is a typo in the fourth equation of the system given in [17])

$$\begin{aligned}\dot{x} &= \lambda - dx - \beta xv,\\ \dot{y} &= \beta xv - ay,\\ \dot{v} &= ky - uv,\\ \dot{w} &= cxyw - cqyw - bw,\\ \dot{z} &= cqyw - hz,\end{aligned} \tag{5}$$

which is based on combining a virus equation to the 4-dimensional model established in [18],

$$\begin{aligned}\dot{x} &= \lambda - dx - \beta xv,\\ \dot{y} &= \beta xv - ay - pyz,\\ \dot{w} &= cxyw - cqyw - bw,\\ \dot{z} &= cqyw - hz.\end{aligned} \tag{6}$$

Note that the second equation in (6) is identical to that of (4), but different from that of (5); and the third equation in (6) is identical to the fourth equation in (5), but different from the third equation in (1) and the fourth equation in (4).

Comparing the two models (4) and (5), we can see that our model (4) is reasonable to have the term $-pyz$ in the second equation (as that used in (6)) since the infected cells are cleared by the CTLes, and then the different term in the fourth equation of (5), $cxyw$, can be interpreted via the interaction of the y equation, leading to the term cyw in fourth equation of (4). Moreover, it is easy to check that all the three models (1), (4) and (6) have three equilibrium solutions: infection-free equilibrium, infectious equilibrium without CTL and infectious equilibrium with CTL, while model (5) can only have two equilibrium solutions (the first two), showing that model (5) has a fundamental difference from the other three models, namely, model (5) cannot exhibit the influence of the CTL and is thus improper to model immunity. Thereby, we will use model (4) in this paper to give a detailed analysis. The notations for the parameters with their units (which are used in systems (1), (4)–(6)) are shown in Table 1. The typical values of these parameters, used in [9] will be given in Section 5 for simulations.

The methodologies used in this paper to analyze model (4) are similar to that used for a 5-dimensional HIV-1 model [19], which introduced a new virus into model (3) to fight the virus [20], described by

Table 1
Definition of the parameter used in model (4).

Parameter	Definition	Unit
λ	Target cell type 1 production rate	cells/ml/day
d	Target cell type death rate	1/day
β	Target cell type 1 infection rate	ml/virion/day
a	Infected cell death rate	1/day
p	Immune-induced clearance rate for infected cells	ml/cell/day
k	Virions production rate for each infected cell	virion/cell/day
u	Virus natural death rate	1/day
c	Production rate of immune system cells correspond to the amount of infected cells (both CTLes and CTLps)	ml/cell/day
q	Ratio of CTLes for each immune system cells produced	(no unit)
b	Death rate of CTLps	1/day
h	Death rate of CTLes	1/day

$$\begin{aligned}
\dot{x} &= \lambda - dx - \beta x v,\\
\dot{y} &= \beta x v - ay - \alpha \bar{v} y,\\
\dot{z} &= \alpha \bar{v} y - bz,\\
\dot{v} &= ky - uv,\\
\dot{\bar{v}} &= cz - q\bar{v},
\end{aligned} \tag{7}$$

where x, y and v represent the same meanings as before, while $\bar{v}$ here denotes the injected virus and z stands for the secondly infected cells. A complete dynamical analysis on model (7) is given in [19] to show static bifurcations between three equilibrium solutions, as well as a Hopf bifurcation, leading to periodic oscillations. Later, this model was modified by adding a control variable to the fifth equation of (7) such that this equation becomes $\dot{\bar{v}} = \eta + cz - q\bar{v}$, where η is the injection rate to measure the amount of the input of the introduced virus. A complete study for this controlled model is given in [21], showing the bifurcations between only two equilibrium solutions and the existence of Hopf bifurcation.

The rest of the paper is organized as follows. In the next section, it will be shown that the model (4) is well-posed. Equilibrium solutions of system (4) and their stability conditions are obtained in Section 3. Hopf bifurcation is discussed in Section 4 numerical example is present in Section 5 to illustrate the applicability of theoretical predictions. Finally, discussion and conclusion are given in Section 6.

2. Well-posedness of the model (4)

For a biological model to be physically meaningful, all solutions of the system should be non-negative for any given non-negative initial conditions. We have the following result.

Theorem 1. *Any solution of system (4), $(x(t), y(t), v(t), w(t), z(t))$, is non-negative for $t > 0$ provided that their initial conditions are non-negative, and is bounded.*

Proof. First note from the first equation of (4) that the solution $x(t)$ can be expressed in the variation form:

$$\begin{aligned}
x(t) &= e^{-\int_0^t (d+\beta v(s))ds} x(0) + \lambda \int_0^t e^{-\int_s^t (d+\beta v(\xi))d\xi} ds,\\
w(t) &= w(0) e^{\int_0^t [cy(s)(1-q)-b]ds},
\end{aligned} \tag{8}$$

which clearly indicates that $x(t) > 0\ \forall t > 0$ provided $x(0) \geqslant 0$, and $w(t) \geqslant 0\ \forall t > 0$ if $w(0) \geqslant 0$. Now consider the second and the third equations in (8) as a nonautonomous system for y and v:

$$\begin{aligned}
\dot{y} &= -(a + pz(t))y + \beta x(t) v,\\
\dot{v} &= -uv + ky,
\end{aligned} \tag{9}$$

with $x = x(t) > 0$ being proved above. By Theorem 2.1 (on page 81) in [22], we know that a solution of (9) with $y(0) \geqslant 0$ and $v(0) \geqslant 0$ remains non-negative. The solution for z can be written as

$$z(t) = e^{-ht}\left(z(0) + \int_0^t cqy(s)w(s)e^{hs} ds\right),$$

which clearly shows that $z(t) \geqslant 0,\ \forall t > 0$ if $z(0) \geqslant 0$ because $y(t) \geqslant 0$ and $w(t) \geqslant 0$, as proved above.

Next, we prove that any non-negative solution of system (4) is bounded. First, note from the first equation of (4) that $\dot{x} \leqslant \lambda - dx$, which in turn yields $\limsup_{t\to\infty} x(t) \leqslant \frac{\lambda}{d}$. Then, by adding the first two equations of (4), we obtain

$$\dot{x}+\dot{y}=\lambda-dx-ay-pyz\leqslant\lambda-\tilde{d}_1(x+y),$$

where $\tilde{d}_1=\min\{a,d\}$. Thus, $\limsup_{t\to\infty}(x(t)+y(t))\leqslant\frac{\lambda}{\tilde{d}_1}$, implying that $y(t)$ is bounded for $t>0$. Similarly, using the first three equations of (4), we have

$$\dot{x}+\dot{y}+\frac{a}{2k}\dot{v}=\lambda-dx-ay-pyz+\frac{a}{2k}(ky-uv)=\lambda-dx-\frac{a}{2}y-\frac{au}{2k}v-pyz\leqslant\lambda-\tilde{d}_2\left(x+y+\frac{a}{2k}v\right),$$

where $\tilde{d}_2=\min\{d,\frac{a}{2},u\}$. This implies that $\limsup_{t\to\infty}(x(t)+y(t)+\frac{a}{2k}v(t))\leqslant\frac{\lambda}{\tilde{d}_2}$, and so $v(t)$ is also bounded for $t>0$.

Having shown that x,y and v are bounded, we can now prove by contradiction that w and z are bounded. Let us assume that z is unbounded. Then, from the y equation in (4), we have $\lim_{t\to\infty}y(t)=0$, and then from the w equation in (4) that $\lim_{t\to\infty}w(t)=0$. It thus follows from the z equation in (4) that $\lim_{t\to\infty}z(t)=0$, which contradicts the assumption. So z must be bounded. Similarly, assume that w is unbounded. Based on the boundedness of z and the z equation of (4), we again have $\lim_{t\to\infty}y(t)=0$. In this case, we see from the w equation of (4) that $\lim_{t\to\infty}w(t)=0$ when $\lim_{t\to\infty}y(t)=0$, which gives another contradiction, and thus w is bounded. The above discussions show that there exists a bounded positive invariant region for the system. We define this region as $\Gamma\subset\mathcal{R}^5_+$, and thus finish the proof of Theorem 1. □

3. Equilibrium solution and stability

In this section, we study the equilibrium solutions of system (4) and their stability, as well as possible bifurcations from these equilibrium solutions.

To obtain the equilibrium solutions of system (4), simply setting $\dot{x}=\dot{y}=\dot{v}=\dot{w}=\dot{z}=0$ yields three equilibrium solutions: the infection-free equilibrium, the infectious equilibrium without CTL, and the infectious equilibrium with CTL response, denoted by E_0, E_1 and E_2, respectively, given as follows:

$$\begin{aligned}
E_0&=\left(\frac{\lambda}{d},0,0,0,0\right),\\
E_1&=\left(\frac{au}{\beta k},\frac{(R_0-1)ud}{\beta k},\frac{(R_0-1)d}{\beta},0,0\right)\\
E_2&=\left(\frac{\lambda}{dR_1},\frac{b}{c(1-q)},\frac{kb}{uc(1-q)},\frac{ah(1-q)}{pqbR_1}(R_0-R_1),\frac{a}{pR_1}(R_0-R_1)\right),
\end{aligned}\tag{10}$$

where R_0 is called the basic reproduction number, defined by

$$R_0=\frac{\lambda\beta k}{aud}\tag{11}$$

and

$$R_1=1+\frac{k\beta b}{c(1-q)du}=1+\frac{abR_0}{\lambda c(1-q)}.\tag{12}$$

It can be seen from the expressions of the equilibrium solutions that the infection-free equilibrium, E_0, always exists for any values of parameters. The infectious equilibrium without CTL, E_1, exists (i.e., $E_1\geqslant 0$) if and only if $R_0\geqslant 1$, while the infectious equilibrium with CTL response, E_2, exists (i.e., $E_2\geqslant 0$) if and only if $R_0\geqslant R_1$.

To determine the stability of the equilibrium solutions, we use the Jacobian matrix of system (4), evaluated at an equilibrium solution, and then consider its characteristic equation. The Jacobian matrix of system (4) is given by

$$J(E)=\begin{bmatrix}
-(d+\beta v) & 0 & -\beta x & 0 & 0\\
\beta v & -(a+pz) & \beta x & 0 & -py\\
0 & k & -u & 0 & 0\\
0 & cw(1-q) & 0 & cy(1-q)-b & 0\\
0 & cqw & 0 & cqy & -h
\end{bmatrix},\tag{13}$$

where E represents any of the equilibrium solution, E_0, E_1 or E_2.

3.1. Infection-free equilibrium E_0

First, we consider the stability of the infection-free equilibrium, E_0, for which we have the following theorem.

Theorem 2. *The infection-free equilibrium solution, E_0, of system (4) is globally asymptotically stable for $R_0<1$.*

Proof. First, we show that the infection-free equilibrium, E_0, is (locally) asymptotically stable. To achieve this, evaluating the Jacobian matrix $J(E)$ at E_0 and computing its characteristic polynomial yield

$$P_0(\xi) = \det[\xi I - J(E_0)] = (\xi + h)(\xi + d)(\xi + b)[\xi^2 + (u + a)\xi + au(1 - R_0)]. \tag{14}$$

The equilibrium E_0 is asymptotically stable if and only if all the roots of the characteristic polynomial, $P_0(\xi)$, have negative real part. $P_0(\xi)$ contains three linear polynomials and a quadratic polynomial. Since all the parameters are positive, the three linear polynomials give negative real roots. So we only need to consider the quadratic polynomial $\xi^2 + (u + a)\xi + au(1 - R_0)$, which is a stable polynomial [23,24] if $au(1 - R_0) > 0$ (since $u + a > 0$), i.e., $R_0 < 1$. Therefore, the infection-free equilibrium, E_0, is asymptotically stable for $R_0 < 1$.

Next, we want to show that the equilibrium E_0 is also globally asymptotically stable for $R_0 < 1$. Here, the method of fluctuation lemma [25] will be used. To apply this method, we introduce the following notations. For any continuous and bounded function $f : [0, \infty) \to R$, denote $f^\infty = \limsup_{t\to\infty} f(t)$ and $f_\infty = \liminf_{t\to\infty} f(t)$. Since the solutions $x(t), y(t), v(t), w(t)$ and $z(t)$ are all non-negative and bounded for non-negative initial conditions, the limits $\limsup_{t\to\infty}$ and $\liminf_{t\to\infty}$ always exist for each of the solutions $x(t), y(t), v(t), w(t)$ and $z(t)$. By the fluctuation lemma, there exists a sequence t_n such that $t_n \to \infty$ as $n \to \infty$, and

$$\lim_{n\to\infty} x(t_n) = x^\infty \quad \text{and} \quad \lim_{n\to\infty} \dot{x}(t_n) = 0.$$

Then substituting t with t_n in the first equation of (4) gives

$$\dot{x}(t_n) + dx(t_n) + \beta x(t_n) v(t_n) = \lambda$$

and taking limit as $n \to \infty$ in the above equation results in

$$d \lim_{n\to\infty} x(t_n) + \beta \lim_{n\to\infty} x(t_n) \lim_{n\to\infty} v(t_n) = \lambda \tag{15}$$

and so

$$dx^\infty \leqslant (d + \beta v_\infty) x^\infty \leqslant \lambda,$$

which asserts that $x^\infty \leqslant \frac{\lambda}{d}$. Next, we apply a similar procedure to the other equations in (4) to obtain the following inequalities:

$$\begin{aligned} &ay^\infty \leqslant (a + pz_\infty) y^\infty \leqslant \beta x^\infty v^\infty, \\ &uv^\infty \leqslant ky^\infty, \\ &bw^\infty \leqslant c(1 - q) y^\infty w^\infty, \\ &hz^\infty \leqslant cqy^\infty w^\infty. \end{aligned} \tag{16}$$

Now we want to prove that $v^\infty = 0$ by using the argument of contradiction. Suppose $v^\infty > 0$. Then, it follows from the above inequalities that

$$\frac{au}{k} v^\infty \leqslant \beta x^\infty v^\infty \leqslant \frac{\lambda\beta}{d} v^\infty, \quad \text{i.e.,} \quad \frac{au}{k}(1 - R_0) v^\infty \leqslant 0 \quad \Rightarrow \quad R_0 \geqslant 1, \tag{17}$$

which contradicts the condition $R_0 < 1$. Hence $v^\infty = 0$, which in turn results in $y^\infty = w^\infty = z^\infty = 0$, and so $v_\infty = y_\infty = w_\infty = z_\infty = 0$. These results imply that $\lim_{t\to\infty} y(t) = \lim_{t\to\infty} v(t) = \lim_{t\to\infty} w(t) = \lim_{t\to\infty} z(t) = 0$. Thus, we obtain the asymptotic differential equation from the first equation of (4) as $\dot{x} = \lambda - dx$, which clearly shows that the solution $x(t) \to \frac{\lambda}{d}$ as $t \to \infty$.

The proof is complete. □

3.2. Infectious equilibrium without CTL response E_1

When the system parameters are varied such that R_0 crosses the critical value 1, the infection-free equilibrium solution, E_0, becomes unstable and the infectious equilibrium solution without CTL, E_1, bifurcates from the transcritical point $R_0 = 1$, at which E_0 and E_1 exchange their stability. Similarly, we have the following stability result for the infectious equilibrium without CTL response, E_1.

Theorem 3. *The infectious equilibrium without* CTL *response,* E_1, *of system* (4) *is globally asymptotically stable for* $1 < R_0 < R_1$.

Proof. To consider the stability of E_1, evaluating the Jacobian matrix $J(E)$ at E_1 yields the characteristic equation, given by

$$P_1(\xi) = \det[\xi I - J(E_1)] = (\xi + h)\left[\xi + \frac{(1 - q)c\lambda}{aR_0}(R_1 - R_0)\right] \times \left[\xi^3 + (a + u + dR_0)\xi^2 + (a + u)dR_0\xi + aud(R_0 - 1)\right], \tag{18}$$

which consists of two linear polynomials and one 3rd-degree polynomial. In order for all the roots of the equation $P_1(\xi)=0$ to have negative real part, it requires that $R_0>1$ (from the constant term of the 3rd-degree polynomial) and $R_0<R_1$ (from the constant term of the quadratic polynomial), and a third condition comes from the 3rd-degree polynomial [17,23]:

$$\begin{aligned}&(a+u+dR_0)(a+u)dR_0-aud(R_0-1)>0\\ \Longleftrightarrow\quad &(a+u)d^2R_0^2+(a^2+u^2)dR_0+adu(R_0+1)>0,\end{aligned}$$

which is satisfied since all parameters take positive values. Thus, the infectious equilibrium without CTL, E_1, is asymptotically stable for $1<R_0<R_1$.

Next, we want to prove that E_1 is also globally asymptotically stable for $1<R_0<R_1$, by using the Lyapunov function method [9,19,26]. To make the notations simpler, we denote E_1 as

$$E_1=(\hat{x},\hat{y},\hat{v},0,0). \tag{19}$$

Then, we construct the Lyapunov function,

$$V=\tilde{m}\left[x-\hat{x}-\hat{x}\ln\frac{x}{\hat{x}}+y-\hat{y}-\hat{y}\ln\frac{y}{\hat{y}}+\frac{a}{k}\left(v-\hat{v}-\hat{v}\ln\frac{v}{\hat{v}}\right)\right]+m(w+z) \tag{20}$$

where $\tilde{m}$ and m are positive coefficients to be determined. It is clear that $V(E_1)=0$, showing that E_1 is the unique global minimum of the Lyapunov function. In the following, we will show that this equilibrium E_1 is globally attractive. To achieve this, taking the derivative of V with respect to time t, along the trajectory of system (4), yields (noticing that $a\hat{y}=\frac{au}{k}\hat{v}=\beta\hat{x}\hat{v}$)

$$\begin{aligned}\left.\frac{dV}{dt}\right|_{(7)}&=\tilde{m}\left[\dot{x}-\frac{\hat{x}}{x}\dot{x}+\dot{y}-\frac{\hat{y}}{y}\dot{y}+\frac{a}{k}\left(\dot{v}-\frac{\hat{v}}{v}\dot{v}\right)\right]+m(\dot{w}+\dot{z})\\
&=\tilde{m}\left[\lambda-dx-\beta xv-\frac{\lambda}{x}\hat{x}+d\hat{x}+\beta\hat{x}v+\beta xv-ay-pyz-\frac{\beta xv}{y}\hat{y}+a\hat{y}+pz\hat{y}+\frac{a}{k}\left(ky-uv-\frac{ky}{v}\hat{v}+u\hat{v}\right)\right]\\
&\quad+m(cyw-bw-hz)\\
&=\tilde{m}\left[\lambda-dx-\frac{\lambda\hat{x}}{x}+d\hat{x}+\left(\beta\frac{au}{\beta k}v-\frac{au}{k}v\right)+\left(a\hat{y}+\frac{au}{k}\hat{v}\right)-\frac{\beta xv\hat{y}}{y}-\frac{ay\hat{v}}{v}\right]-\tilde{m}pz(y-\hat{y})+m(cyw-bw-hz)\\
&=\tilde{m}\left[\lambda-dx-\frac{\lambda\hat{x}}{x}+d\hat{x}+2\beta\hat{x}\hat{v}-\frac{\beta xv\hat{y}}{y}-\frac{ay\hat{v}}{v}\right]-[mh+\tilde{m}p(y-\hat{y})]z+mc\left(y-\frac{b}{c}\right)w\\
&\leqslant-[mh+\tilde{m}p(y-\hat{y})]z+mc\left(y-\frac{b}{c}\right)w,\end{aligned}$$

where the first term in the square bracket being non-positive is proved as follows:

$$\begin{aligned}\lambda-dx-\frac{\lambda\hat{x}}{x}+d\hat{x}+2\beta\hat{x}\hat{v}-\frac{\beta xv\hat{y}}{y}-\frac{ay\hat{v}}{v}&=\lambda-dx-\frac{\lambda\hat{x}}{x}+d\hat{x}-\beta\hat{x}\hat{v}+\beta\hat{x}\hat{v}\frac{\hat{x}}{x}+3\beta\hat{x}\hat{v}-\beta\hat{x}\hat{v}\frac{\hat{x}}{x}-\frac{\beta xv\hat{y}}{y}-\frac{ay\hat{v}}{v}\\
&=\left(1-\frac{\hat{x}}{x}\right)(\lambda-\beta\hat{x}\hat{v}-dx)-\beta\hat{x}\hat{v}\left(\frac{\hat{x}}{x}+\frac{xv\hat{y}}{\hat{x}\hat{v}y}+\frac{ay}{\beta\hat{x}v}-3\right)\\
&=\left(1-\frac{\hat{x}}{x}\right)\left[dR_0\hat{x}-\beta\hat{x}\frac{(R_0-1)d}{\beta}-dx\right]-\beta\hat{x}\hat{v}\left(\frac{\hat{x}}{x}+\frac{xv\hat{y}}{\hat{x}\hat{v}y}+\frac{ay}{\beta\hat{x}v}-3\right)\\
&=-\frac{d}{x}(x-\hat{x})^2-\beta\hat{x}\hat{v}\left(\frac{\hat{x}}{x}+\frac{xv\hat{y}}{\hat{x}\hat{v}y}+\frac{ay}{\beta\hat{x}v}-3\right)\\
&\leqslant-\frac{d}{x}(x-\hat{x})^2-\beta\hat{x}\hat{v}\left[3\left(\frac{\hat{x}}{x}\frac{xv\hat{y}}{\hat{x}\hat{v}y}\frac{ay}{\beta\hat{x}v}\right)^{1/3}-3\right]\\
&=-\frac{d}{x}(x-\hat{x})^2-\beta\hat{x}\hat{v}\left[3\left(\frac{a\hat{y}}{\beta\hat{x}\hat{v}}\right)^{1/3}-3\right]=-\frac{d}{x}(x-\hat{x})^2\leqslant 0,\end{aligned}$$

where the well-known inequality $a+b+c\geqslant 3(abc)^{1/3}$ $(a>0,b>0,c>0)$ has been used.

In order to show $\frac{dV}{dt}<0$, note that for different values of y relative to $\hat{y}$ and $\frac{b}{c}$, we can define the positive constants $\tilde{m}$ and m to scale the different expressions properly to ensure that the inequality holds. For most cases, the scaling can be performed directly based on the bounds on the variables. We first assume $y>\hat{y}$. In this case, we only need to consider $y>\frac{b}{c}$ and we need to ensure that $\lim_{t\to\infty}z(t)=0$ does not happen before $\lim_{t\to\infty}w(t)=0$ does. As $z\to 0$ when $t\to\infty$, the equation $\dot{w}+\dot{z}=(cy-b)w-hz$ approaches $\dot{w}=(cy-b)w$. Given that $y-\frac{b}{c}>0$, w will grow unboundedly, which contradicts that the system is well-posed. Hence, as z approaches zero, w must also approaches zero. Therefore, $w>0$ must result in $z>0$, and thus for the terms $-\tilde{m}p(y-\hat{y})z+mc(y-\frac{b}{c})w$, we can choose $\tilde{m}\gg m$, so that $\frac{dV}{dt}<0$. This result implies that the trajectory enters the region bounded by $y<\hat{y}+\varepsilon$ at some finite time $T_1>0$ and then it will stay in this region for $t\in[T_1,\infty)$. Moreover, we have

$$\frac{b}{c(1-q)}-\hat{y}=\frac{b}{c(1-q)}-\frac{(R_0-1)ud}{\beta k}=\frac{ud}{\beta k}\left(1+\frac{b\beta k}{cdu(1-q)}-R_0\right)=\frac{ud}{\beta k}(R_1-R_0)>0 \quad \text{for } 1<R_0<R_1,$$

implying that we can always choose appropriate $\tilde{m}$ and m to ensure that $\frac{b}{c(1-q)}>\hat{y}>y-\epsilon$, i.e., $y<\frac{b}{c(1-q)}+\varepsilon$ for arbitrary small ε. So at some finite time $T_2>T_1$, the solution trajectory must enter the region $y\leqslant\frac{b}{c(1-q)}$ and stay there for $t\in[T_2,\infty)$.

Having shown that y must be bounded above by $\frac{b}{c(1-q)}$ in finite time, we can now prove that the solution trajectory will converge E_1 asymptotically. First, it follows from the third equation of (16) that

$$bw^{\infty}\leqslant c(1-q)y^{\infty}w^{\infty} \quad \text{or} \quad \left(\frac{b}{c(1-q)}-y^{\infty}\right)w^{\infty}\leqslant 0.$$

Then for $t\in[T_2,\infty)$, the above inequality only holds if $w^{\infty}=0$ and thereby $z^{\infty}=0$, which yields asymptotic dynamical system as follows:

$$\begin{aligned}\dot{x}&=\lambda-dx-\beta xv,\\ \dot{y}&=\beta xv-ay,\\ \dot{v}&=ky-uv.\end{aligned}\tag{21}$$

The subsystem (21) has two equilibria,

$$\hat{E}_0=\left(\frac{\lambda}{d},0,0\right) \quad \text{and} \quad \hat{E}_1=(\hat{x},\hat{y},\hat{v}),$$

where $(\hat{x},\hat{y},\hat{v})$ is defined in (19). It is easy to show that for $1<R_0<R_1$, $\hat{E}_0$ is unstable and $\hat{E}_1$ is asymptotically stable. To prove that $\hat{E}_1$ is also globally asymptotically stable, we construct a Lyapunov function, given by

$$\hat{V}=x-\hat{x}-\hat{x}\ln\frac{x}{\hat{x}}+y-\hat{y}-\hat{y}\ln\frac{y}{\hat{y}}+\frac{a}{k}\left(v-\hat{v}-\hat{v}\ln\frac{v}{\hat{v}}\right)\tag{22}$$

and similarly we may show that

$$\left.\frac{d\hat{V}}{dt}\right|_{(21)}\leqslant 3\beta\hat{x}\hat{v}\left[1-\left(\frac{a\hat{y}}{\beta\hat{x}\hat{v}}\right)^{1/3}\right]=0,\tag{23}$$

with the equality to hold only if $(x,y,v)=(\hat{x},\hat{y},\hat{v})$. So for $1<R_0<R_1$, the equilibrium $\hat{E}_1$ of the subsystem (21) is globally asymptotically stable, from which we can conclude that the equilibrium E_1 of the original system (4) is globally asymptotically stable.

The proof of Theorem 3 is finished. □

3.3. Infectious equilibrium with CTL response E_2

Now we consider the infectious equilibrium with CTL response, E_2. Suppose the system parameters are varied such that R_0 crosses the critical value R_1 at which the equilibrium without CTL response, E_1, becomes unstable and bifurcates into the equilibrium with CTL response, E_2. In the following, we assume $R_0>R_1$. In order to simplify the analysis for the equilibrium E_2, we first take the following scaling on the state variables, parameters and time,

$$\begin{aligned}&x\to\frac{\lambda}{\phi}x, \quad y\to\frac{\lambda}{\phi}y, \quad v\to\frac{\phi}{\beta}v, \quad w\to\frac{k\beta}{cpq}w, \quad z\to\frac{\phi}{p}z,\\ &\frac{a}{\phi}\to a, \quad \frac{b}{\phi}\to b, \quad \frac{h}{\phi}\to h, \quad \frac{d}{\phi}\to d, \quad \frac{u}{\phi}\to u, \quad \frac{c(1-q)\lambda}{\phi^2}\to c,\\ &\phi=\sqrt[3]{\lambda\beta k}, \quad t=\frac{\tau}{\phi},\end{aligned}$$

which results in the scaled system:

$$\begin{aligned}\frac{dx}{d\tau}&=1-dx-xv,\\ \frac{dy}{d\tau}&=xv-ay-yz,\\ \frac{dv}{d\tau}&=y-uv,\\ \frac{dw}{d\tau}&=cyw-bw,\\ \frac{dz}{d\tau}&=yw-hz.\end{aligned}\tag{24}$$

Now for system (24), the R_0 and R_1 become

$$R_0 = \frac{1}{aud}, \quad R_1 = 1 + \frac{b}{cud} \tag{25}$$

and the equilibrium solution E_2 becomes

$$E_2 = \left(\frac{1}{dR_1}, \frac{b}{c}, \frac{b}{cu}, \frac{ach(R_0 - R_1)}{bR_1}, \frac{a(R_0 - R_1)}{R_1}\right).$$

The Jacobian matrix of system (24) evaluated at E_2 is

$$J(E) = \begin{bmatrix} -dR_1 & 0 & -\frac{1}{dR_1} & 0 & 0 \\ \frac{b}{cu} & -\frac{aR_0}{R_1} & \frac{1}{dR_1} & 0 & -\frac{b}{c} \\ 0 & 1 & -u & 0 & 0 \\ 0 & \frac{ac^2h}{b}\left(\frac{R_0}{R_1} - 1\right) & 0 & 0 & 0 \\ 0 & \frac{ach}{b}\left(\frac{R_0}{R_1} - 1\right) & 0 & \frac{b}{c} & -h \end{bmatrix} \tag{26}$$

from which we obtain the characteristic polynomial, given by

$$\det(\xi I - J) = \xi^5 + a_1\xi^4 + a_2\xi^3 + a_3\xi^2 + a_4\xi + a_5, \tag{27}$$

where

$$\begin{aligned} a_1 &= u + h + dR_1 + \frac{aR_0}{R_1}, \\ a_2 &= \frac{1}{u} + uh + (u + h)dR_1 + ah\left(\frac{2R_0}{R_1} - 1\right), \\ a_3 &= \frac{h}{u} + hduR_1 + \frac{abR_0}{cR_1} + ah(b + u + dR_1)\left(\frac{R_0}{R_1} - 1\right), \\ a_4 &= ah\left\{\frac{bR_0}{cR_1} + [bu + d(b + u)R_1]\left(\frac{R_0}{R_1} - 1\right)\right\}, \\ a_5 &= bh\left(1 - \frac{R_1}{R_0}\right). \end{aligned} \tag{28}$$

It is obvious that all a_i's are positive for $R_0 > R_1$. According to the Hurwitz condition [23,24], the necessary and sufficient conditions for the equilibrium E_2 to be asymptotically stable are: $\Delta_i > 0,\ i = 1, 2, \ldots, 5$, where

$$\begin{aligned} \Delta_1 &= a_1, \\ \Delta_2 &= a_1a_2 - a_3, \\ \Delta_3 &= a_3\Delta_2 - a_1(a_1a_4 - a_5), \\ \Delta_4 &= a_4\Delta_3 - a_5[a_2\Delta_2 - (a_1a_4 - a_5)], \\ \Delta_5 &= a_5\Delta_4. \end{aligned} \tag{29}$$

To verify if $\Delta_2 > 0$, a direct, tedious calculation shows that

$$\begin{aligned} \Delta_2 = {} & 1 + uh(u + h) + \frac{2h}{u} + \frac{(2h + u)R_1}{aR_0} + \frac{2h + d}{dR_1} + \frac{aR_0}{uR_1} + \frac{d(1 + uh^2)R_1}{u} + \frac{dR_1^2}{aR_0} + d^2hR_1^2 + ah^2\left(\frac{2R_0}{R_1} - 1\right) \\ & + a^2h\frac{R_0}{R_1}\left(\frac{2R_0}{R_1} - 1\right) + abh\left(1 - \frac{R_0}{R_1}\right). \end{aligned} \tag{30}$$

Note that the last term in Δ_2 is negative. So we cannot conclude that $\Delta_2 > 0$ for all positive parameter values. Nevertheless, we can show that Δ_3 crosses zero before Δ_2 does, as shown in the following. Hence, the violation of the stability conditions for the equilibrium E_2 will happen on Δ_3 before on Δ_2. As a matter of fact, we have

Lemma 1. *If Δ_2 and Δ_3 can change their signs from positive to negative when R_0 is increasing from R_1, then Δ_3 will change its sign before Δ_2 does.*

Proof. To show this, we first prove that when $\Delta_2 = 0, \Delta_3$ has already been negative. Under $\Delta_2 = 0, \Delta_3$ is simplified to

$$\Delta_3 = -a_1(a_1a_4 - a_5).$$

Since $a_1 > 0$ and a direct calculation shows that

$$a_1a_4-a_5=ah\left[\frac{bR_0}{cR_1}+du(R_0-R_1)\right]\left(u+h+dR_1+\frac{aR_0}{R_1}\right)+abh(u+dR_1)\left(\frac{R_0}{R_1}-1\right)\left(u+h+dR_1+\frac{aR_0}{R_1}\right)-bh\left(1-\frac{R_1}{R_0}\right)$$
$$=ah\left\{\left[\frac{bR_0}{cR_1}+du(R_0-R_1)\right]\left(u+h+dR_1+\frac{aR_0}{R_1}\right)+b(u+dR_1)\left(\frac{R_0}{R_1}-1\right)\left(h+dR_1+\frac{aR_0}{R_1}\right)+bu^2\left(\frac{R_0}{R_1}-1\right)\right\}>0, \quad (31)$$

$\Delta_3=-a_1(a_1a_4-a_5)<0$ holds when $\Delta_2=0$. On the other hand, when $\Delta_3=0,\Delta_2$ is still positive, since the equation $\Delta_3=0$ yields (see the third equation in (29))

$$\Delta_2=\frac{a_1}{a_3}(a_1a_4-a_5)>0,$$

implying that Δ_3 must cross zero before Δ_2 does. □

Similarly, for Δ_3 and Δ_4, we have the following result.

Lemma 2. *If Δ_3 and Δ_4 can change their sings from positive to negative as R_0 is increasing from R_1, then Δ_4 becomes negative before Δ_3 does.*

Proof. We need to show that when $\Delta_3=0,\Delta_4$ must have been negative, and when $\Delta_4=0,\Delta_3$ can still be positive. First, using the condition $\Delta_3=0$, we obtain

$$\Delta_3=a_3\Delta_2-a_1(a_1a_4-a_5)=0 \quad \Rightarrow \quad a_1a_4-a_5=\frac{a_3}{a_1}\Delta_2$$

and thus

$$\Delta_4=-a_5\left(a_2\Delta_2-\frac{a_3}{a_1}\Delta_2\right)=-\frac{a_5}{a_1}\Delta_2^2<0.$$

On the other hand, suppose $\Delta_4=0$ from which we use the fourth equation of (29) to obtain

$$\Delta_3=\frac{a_5}{a_4}[a_2\Delta_2-(a_1a_4-a_5)].$$

Then it follows from the third equation of (29) that

$$a_1a_4-a_5=\frac{1}{a_1}(a_3\Delta_2-\Delta_3),$$

which is then substituted into the above equation to solve for Δ_3, yielding

$$\Delta_3=\frac{\frac{a_5}{a_4}\left(a_2-\frac{a_3}{a_1}\right)\Delta_2}{1-\frac{a_5}{a_1a_4}}=\frac{a_5\Delta_2^2}{a_1a_4-a_5}>0 \quad (\text{since } a_1a_4-a_5>0).$$

Combining the above two steps indicates that Δ_4 changes its sign from positive to negative before Δ_3 does. □

Remark 1. Lemmas 1 and 2 indicate the order of violation of stability for the equilibrium E_2 is Δ_4,Δ_3 and then Δ_2.

In fact, at $R_0=R_1$, (30) shows that $\Delta_2>0$, and Δ_3 and Δ_4 can be simplified as

$$\Delta_3|_{R_0=R_1}=a_3\Delta_2-a_1^2a_4|_{b=\frac{c}{a}-cud,\ 0<aud<1}$$
$$=\frac{1}{a^3u^3}\left[a+u+au(a^2+u^2+au+da^2u^2)\right]\times\left\{h\left[h+a+u+au(a+u)h+auh^2\right]+au(1-aud)\right\}>0,$$

$$\Delta_4|_{R_0=R_1}=\frac{abh}{c}\Delta_3|_{R_0=R_1}>0.$$

Thus, since $\Delta_2,\Delta_3,\Delta_4$ depend continuously on the parameters, we can assert that at least in a small neighborhood of R_1, for $R_0>R_1,\Delta_2,\Delta_3$ and Δ_4 are all positive, while Δ_5 is always positive for $R_0>R_1$. The above result gives the following theorem.

Theorem 4. *There is an $R_2>R_1$ such that when $R_0\in(R_1,R_2)$, the equilibrium E_2 is asymptotically stable. When R_0 continues increasing, Δ_4 may first become negative and thus E_2 becomes unstable and a bifurcation emerges from E_2.*

4. Hopf Bifurcation

Finally, we consider possible bifurcation which occurs from the equilibrium E_2. It follows from Lemmas 1 and 2 that the only possible bifurcation occurs from E_2 at the critical point defined by $\Delta_4=0$. In order to classify the bifurcation at $\Delta_4=0$. we need the following result [23].

Lemma 3. [23] *Consider the general nonlinear system, described by the following differential equation:*

$$\dot{x} = f(x,\mu), \quad x \in R^n, \quad \mu \in R^m \quad f : R^{n+m} \to R^n.$$

It is assumed that $f(0,\mu) = 0$, i.e., $x = 0$is an equilibrium solution for any values of μ, and the nonlinear function f is analytic. Then, the necessary and sufficient condition for this system to have a Hopf bifurcation from $x = 0$ is $\Delta_{n-1} = 0$.

Now, for our system (21), by Lemmas 1 and 2, the only bifurcation from the equilibrium E_2 is Hopf bifurcation, which occurs at $\Delta_4 = 0$. Thus, the existence of a Hopf bifurcation from the E_2 is equivalent to the existence of $\Delta_4 = 0$. We have the following result.

Theorem 5. *For some large value of c and small value of a, there exist other parameter values satisfying $R_0 > R_1$ and $\Delta_4 = 0$, at which the equilibrium E_2 loses its stability and a Hopf bifurcation occurs, which gives rise to a family of limit cycles.*

Proof. We have known that $\Delta_4 > 0$ at $R_0 = R_1$. Thus, when R_0 is increasing from $R_0 = R_1$, in order to have a Hopf bifurcation, Δ_4 must become negative at some value of $R_0 > R_1$. Noticing that $R_0 = \frac{1}{aud}$ and $R_1 = 1 + \frac{b}{cud}$, one may choose small value of a and large value of c, under which $R_0 \to \infty$ while $R_0 > R_1$ still holds. Therefore, we can pick up a small value for a and a large value for c, and thus obtain the Laurent expansion of Δ_4 with respect to c as

$$\Delta_4 = \frac{h}{u^4 c^3 (b + cud)^3}(C_7 c^7 + C_6 c^6 + \cdots + C_0) + O(a),$$

whose leading term coefficient, with respect to c, is C_7, given by

$$C_7 = -u^4\left[ud^5 + u(h+u)d^4 + (1+hu^2)d^3 + 2hd^2 + h(bd + bu + ud)\right](a_2 b^2 + a_1 b + a_0),$$

which shows that the sign of the leading term of Δ_4, C_7, is determined by the sign of the quadratic polynomial $a_2 b^2 + a_1 b + a_0$, where

$$\begin{aligned} a_2 &= duh, \\ a_1 &= u^4(u+h)d^2 + u(2u^2 + uh - 2h^2)d + u - 2h, \\ a_0 &= -hu\left[u^3(u+h)d^2 + 2u(u+h)d + 2\right]. \end{aligned}$$

Since $a_2 > 0$, $a_0 < 0$, the quadratic polynomial has two real roots b_1 and b_2 satisfying $b_1 < 0 < b_2$. Thus, choosing $b > b_2$ yields $a_2 b^2 + a_1 b + a_0 > 0$, and so $C_7 < 0$, leading to $\Delta_4 < 0$, which finishes the proof by using Lemma 3. □

Certainly, the conditions given in the above proof (taking small value of a and large value of c) are sufficient, but not necessary. We will show in the next section, that Δ_4 can reach zero even when a not very small value of a is selected. Having proved the existence of Hopf bifurcation from the equilibrium E_2, in the next section, we will choose one parameter as the bifurcation parameter and use normal form theory to analyze the stability of bifurcating limit cycles. Also, we will use numerical simulation to verify the theoretical results.

5. Numerical illustrations

In this section, we present a numerical example to demonstrate the theoretical results obtained in the previous sections. For simulation, we use the original system (4) whose system parameters have direct physical meaning. We consider the dynamics of the system as the basic reproduction number, R_0, is increasing. For convenience, we choose λ as a bifurcation parameter and fix all other parameter values. We have noticed that the parameter values, $d = c = h = q = 0.1, a = 0.5, p = 1$, are used in [14] and adapted later in [9] (noting that they are different from that used in [19] since the scaled system is used for simulation in [19]). Two values of $b, 0.001$ and 0.2 are used in [14], indicating that the range of the values of b is quite large. The value $b = 0.2$ is used in [9]. The value of β used in [14] is $\beta = 0.001$, while that used in [9] is $\beta = 0.0075$, which may be reasonable since the β used in another HIV model [20] is $\beta = 0.004$. According to [15], the parameters k and u take the values $k = 100$ and $u \geqslant 3$, and the values of these two parameters used in [20] are $k = 50$ and $u = 2$, which are comparable to that used in [15]. Moreover, it was discussed in [17] that $u \gg a$. In order to make the simulation give a good comparison with that shown in [9], we take the same parameter values used in [9] and choose appropriate values for k and u as follows (with the units shown in Table 1):

$$d = c = h = q = \frac{1}{10}, \quad a = \frac{1}{2}, \quad p = 1, \quad b = \frac{1}{5}, \quad \beta = \frac{3}{400}, \quad k = 25, \quad u = 8. \tag{32}$$

It has been noted that the values of λ used for simulations in [13] is $\lambda = 1$, in [14] is $\lambda = 10$, and in [20] is $\lambda = 2$. This indicates that the values of λ have a fairly large variation. In this paper, adding the virus equation to the system makes the model more realistic and the simulation results will be compared to that obtained in [9].

Under the parameter values given in (32) we have

$$R_0 = \frac{15}{32}\lambda, \quad R_1 = \frac{73}{48}. \tag{33}$$

5.1. Infection-free equilibrium E_0

It is easy to see that when $0 < \lambda < \frac{32}{15}$, $0 < R_0 < 1$. With the parameter values given in (32), letting $\lambda = 1.5$ yields the infection-free equilibrium, $E_0: (x, y, v, w, z) = (15, 0, 0, 0, 0)$ and E_0 is globally asymptotically stable for these given parameter values. The simulation result is shown in Fig. 1, indicating that all state variables, except for x, converge to zero, and x converges to 15. It can be seen that all of them converge in a similar speed, namely, they reach the equilibrium E_0 in a roughly same time frame. However, it is noted that the virus v first increases and then monotonically decreases rapidly, while x monotonically increases and the other three variables monotonically decrease right from the beginning. The initial conditions for all simulations are given by $(x(0), y(0), v(0), w(0), z(0)) = (0.5, 1.5, 0.1, 1.5, 1.5)$.

5.2. Infectious equilibrium without CTL response E_1

When λ is increased such that $1 < R_0 < R_1$, i.e., $\frac{32}{15} < \lambda < \frac{146}{45}$, we choose $\lambda = 2.5$. With the parameter values given in (32), the infectious equilibrium without CTL response becomes, $E_1: (x, y, v, w, z) = (\frac{64}{3}, \frac{11}{15}, \frac{55}{24}, 0, 0)$, which is globally asymptotically stable, as shown in Fig. 2. An interesting phenomenon is observed from x, which is no longer monotonically increasing, like the previous case shown in Fig. 1, but now it increases first to reach a steady-state value for a quite long period, and then decreases to reach its final steady-state value (see Fig. 2). It is also noted that x, y and v converge to their final steady-state values, i.e., the equilibrium E_1 in the same time frame (after about 280 days), while w and z reach the E_1 in about 50 days, which is actually the time for x to reach its first steady-state value.

5.3. Infectious equilibrium with CTL response E_2

When R_0 is further increased such that $R_1 < R_0 < R_H$, where R_H denotes a Hopf critical point, which gives $\frac{146}{45} < \lambda < \lambda_H$, where λ_H represents a Hopf critical point in terms of λ. If we choose $\lambda = 8$, then the equilibrium E_1 becomes unstable and the infectious equilibrium with CTL response bifurcates, and its solution is given by $E_2: (x, y, v, w, z) = (\frac{3840}{73}, \frac{20}{9}, \frac{125}{18}, \frac{963}{292}, \frac{107}{146})$ which is asymptotically stable. The simulation results are shown in Fig. 3. It is seen from this figure that all the state variables now are not monotonically increasing or decreasing, but show oscillating behavior for a quite long period before reaching the equilibrium E_2, in the same time frame.

5.4. Hopf bifurcation

Finally, we investigate the Hopf bifurcation which occurs from the infectious equilibrium with CTL response, E_2. To find the Hopf critical point, we apply the Hurwitz condition in terms of the parameter λ. The characteristic polynomial at E_2 with the given parameter values is $\det(\xi - J) = \xi^5 + a_1\xi^4 + a_2\xi^3 + a_3\xi^2 + a_4\xi + a_5$, where

$$a_1 = \frac{45}{292}\lambda + \frac{3961}{480}, \quad a_2 = \frac{507}{9344}\lambda + \frac{3171}{1600}, \quad a_3 = \frac{9123}{46720}\lambda - \frac{947}{3200},$$
$$a_4 = \frac{23499}{467200}\lambda - \frac{6833}{48000}, \quad a_5 = \frac{3}{800}\lambda - \frac{73}{6000}.$$

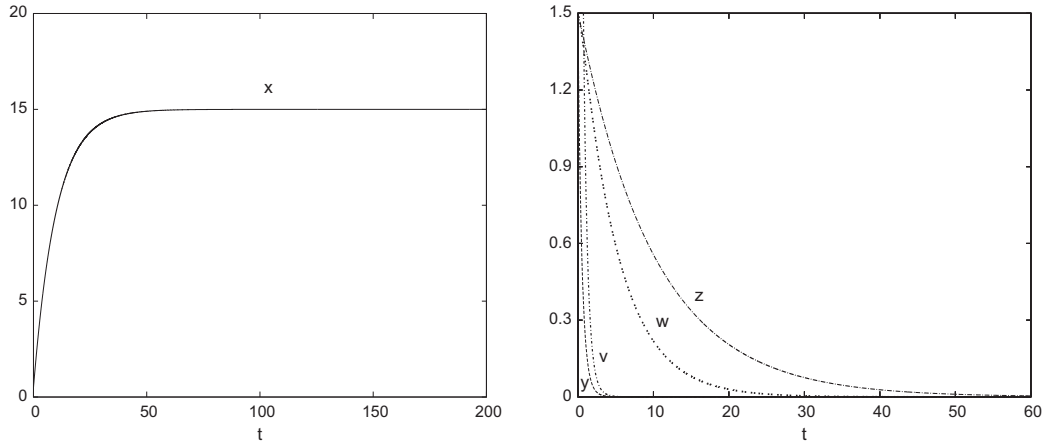

Fig. 1. Simulation of system (4) for the parameter values given in (32) and $\lambda = 1.5$, showing that solution trajectories converge to the infection-free equilibrium, E_0.

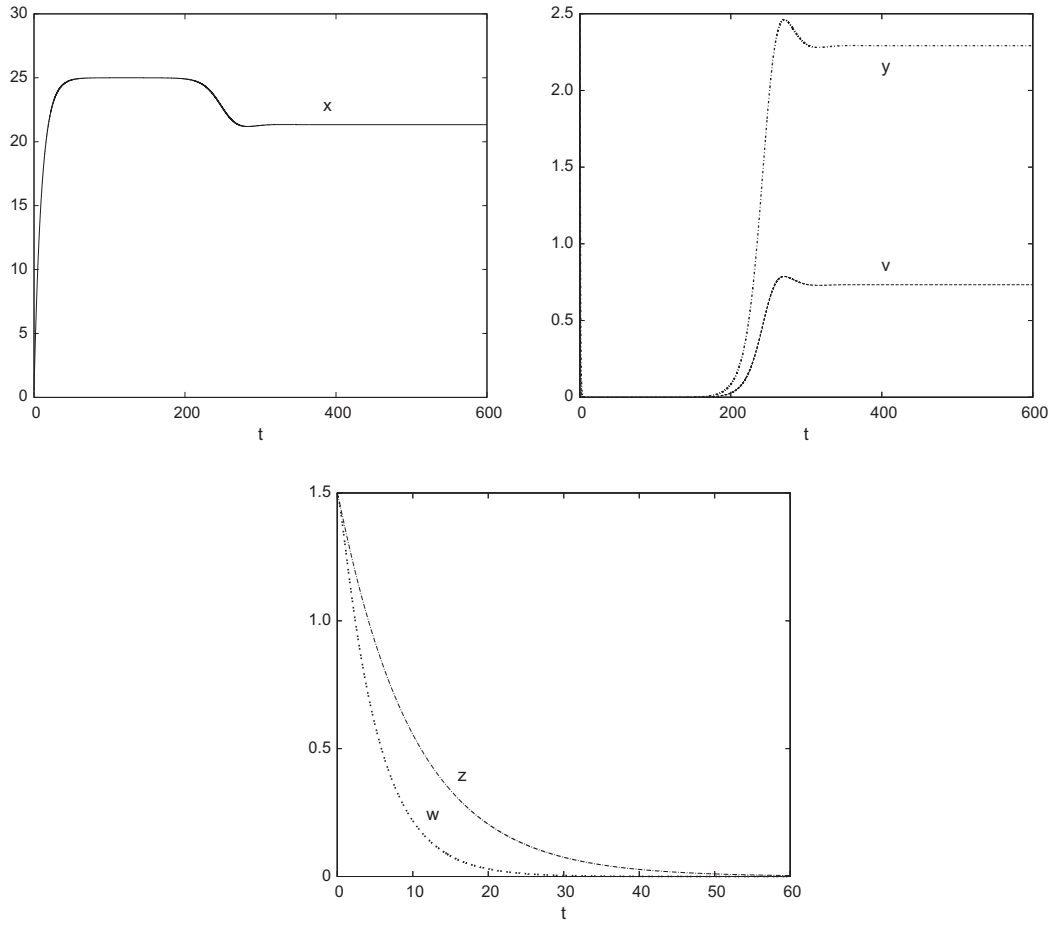

Fig. 2. Simulation of system (4) for the parameter values given in (32) and $\lambda = 2.5$, showing that solution trajectories converge to the infection equilibrium without CTL response, E_1.

It is obvious when $\lambda > R_1 = \frac{73}{48}$, all $a_i > 0, i = 1, 2, \ldots, 5$. Using the formulas given in (29) yields

$$\Delta_2 = \frac{22815}{2728448}\lambda^2 + \frac{834097}{1495040}\lambda + \frac{4262537}{256000},$$
$$\Delta_3 = \frac{11173545}{25494618112}\lambda^3 - \frac{1222500693}{69848268800}\lambda^2 + \frac{250093357}{4784128000}\lambda + \frac{103203490393}{22118400000},$$
$$\Delta_4 = \frac{48460278159}{2382217116385280}\lambda^4 - \frac{35367315203007}{32633111183360000}\lambda^3 - \frac{1067753112051}{2235144601600000}\lambda^2 + \frac{68228290293677}{574095360000000}\lambda - \frac{263916103027577}{1061683200000000}.$$

The equation $\Delta_4 = 0$ has four real roots:

$$\lambda = -10.6429084180, \quad 2.2049072423, \quad 10.0861091266, \quad 51.6288047682.$$

It is easy to use (33) to verify that both $\lambda = 10.0861091266$ and $\lambda = 51.6288047682$ satisfy the requirement, $R_0 > R_1$. This implies that there exist two Hopf critical points: $\lambda_{H_1} = 10.0861091266$, and $\lambda_{H_2} = 51.6288047682$, and the infectious equilibrium with CTL response, E_2, is asymptotically stable for $\lambda \in (\frac{146}{45}, \lambda_{H_1}) \cup (\lambda_{H_2}, \infty)$. We take $\lambda = \lambda_{H_1} = 10.0861091266$ (i.e., $R_0 = 4.7278636531$), and present a detailed analysis on the Hopf bifurcation and bifurcating limit cycles. At $\lambda = \lambda_{H_1}$, the approximate eigenvalues of the characteristic polynomial are

$$\pm 0.3919579290i, \quad -9.5597869096, \quad -0.1233312781 \pm 0.0475216884i.$$

Next, we will use the perturbation method and the Maple program developed in [27] to compute the normal form of system (4) around the critical point $\lambda = \lambda_{H_1}$. The first step is to shift the equilibrium E_2 to the origin and apply a linear transformation such that the linear part of the transformed system is in the Jordan canonical form. Introducing

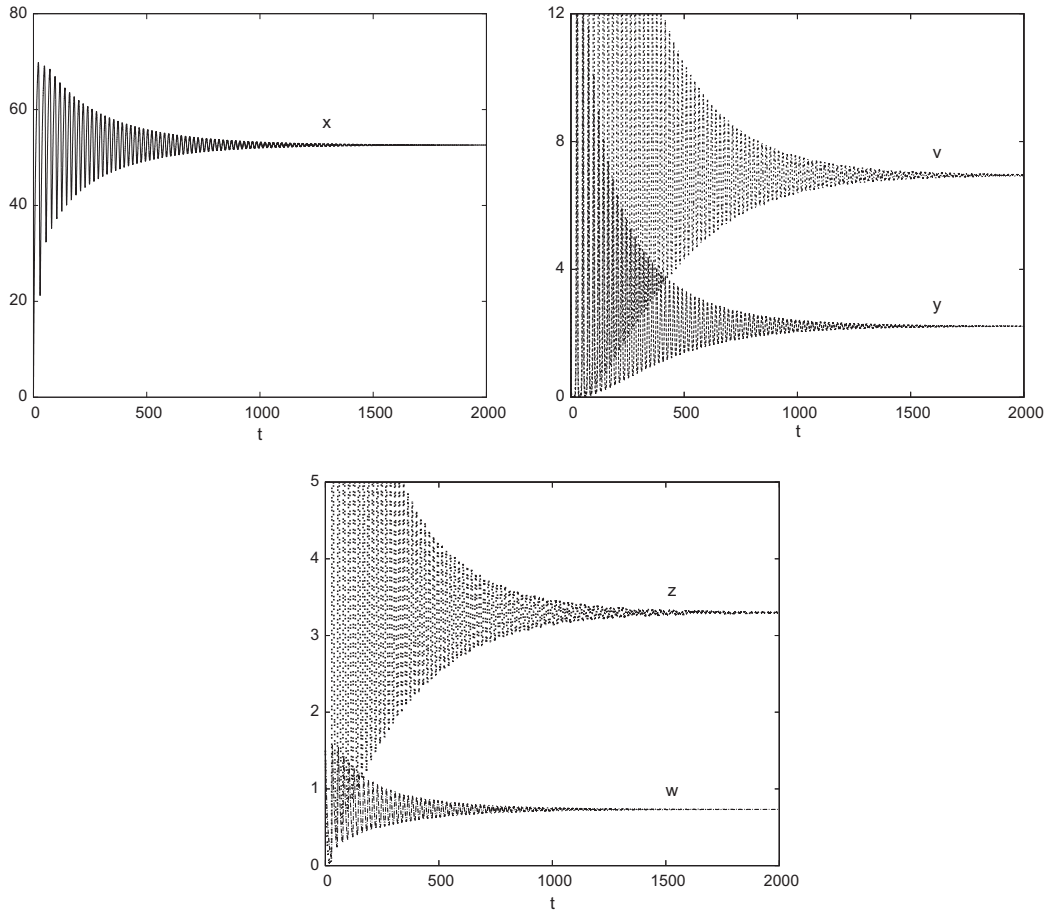

Fig. 3. Simulation of system (4) for the parameter values given in (32) and $\lambda = 8$, showing that solution trajectories converge to the infection equilibrium with CTL response, E_2.

$$\begin{pmatrix} x \\ y \\ v \\ w \\ z \end{pmatrix} = E_2 + T\begin{pmatrix} \tilde{x} \\ \tilde{y} \\ \tilde{v} \\ \tilde{w} \\ \tilde{z} \end{pmatrix} = \begin{pmatrix} 66.3196216542 \\ 2.2222222222 \\ 6.9444444444 \\ 4.7446475963 \\ 1.0543661325 \end{pmatrix} + T\begin{pmatrix} \tilde{x} \\ \tilde{y} \\ \tilde{v} \\ \tilde{w} \\ \tilde{z} \end{pmatrix}, \tag{34}$$

where T is 4×4 non-singular constant matrix, into system (4) yields the following system:

$$\begin{aligned}
\dot{\tilde{x}} &= 0.3919579290\tilde{y} + (-0.0107638681\tilde{x} + 0.0480927093\tilde{y} + \cdots)\mu + f_1(\tilde{x}, \tilde{y}, \tilde{v}, \tilde{w}, \tilde{z}),\\
\dot{\tilde{y}} &= -0.3919579290\tilde{x} + (0.0035065777\tilde{x} + 0.0131021256\tilde{y} + \cdots)\mu + f_2(\tilde{x}, \tilde{y}, \tilde{v}, \tilde{w}, \tilde{z}),\\
\dot{\tilde{v}} &= -9.5597869096\tilde{v} + (\cdots)\mu + f_3(\tilde{x}, \tilde{y}, \tilde{v}, \tilde{w}, \tilde{z}),\\
\dot{\tilde{w}} &= -0.1233312781\tilde{w} + 0.0475216884\tilde{z} + (\cdots)\mu + f_4(\tilde{x}, \tilde{y}, \tilde{v}, \tilde{w}, \tilde{z}),\\
\dot{\tilde{z}} &= -0.0475216884\tilde{w} - 0.1233312781\tilde{z} + (\cdots)\mu + f_5(\tilde{x}, \tilde{y}, \tilde{v}, \tilde{w}, \tilde{z}),
\end{aligned} \tag{35}$$

where $f_i(\tilde{x}, \tilde{y}, \tilde{v}, \tilde{w}, \tilde{z}), i = 1, 2, \ldots, 5$ are homogeneous quadratic polynomials of $\tilde{x}, \tilde{y}, \tilde{v}, \tilde{w}$ and $\tilde{z}$. Note that system (35) now has equilibrium at the origin for any real values of μ. The Jacobian matrix of (35) evaluated at the origin for the critical value $\mu = 0$ is indeed in the Jordan canonical form.

Now, executing the Maple program [27] on the above system, we obtain the following normal form up to third order terms,

$$\begin{aligned}
\dot{r} &= r(v_0\mu + v_1 r^2 + \cdots) = r(0.0011691287\mu - 0.0000950369r^2 + \cdots),\\
\dot{\theta} &= \omega_c + t_0\mu + t_1 r^2 + \cdots = 0.3919579290 + 0.0222930658\mu - 0.0042326886r^2 + \cdots,
\end{aligned} \tag{36}$$

where the v_0 and t_1 are obtained via the linear analysis on system (35) with the following formulas [28]:

$$v_0 = \frac{1}{2}(-0.0107638681 + 0.0131021256)\mu = 0.0011691287\mu,$$
$$t_0 = \frac{1}{2}(0.0480927093 - 0.0035065777)\mu = 0.0222930658\mu$$

and v_1 and t_1 are obtained from the output of the Maple program.

The normal form (36) can be used to analyze the stability of bifurcating periodic solutions. Letting $\dot{r} = 0$ yields two steady-state solutions: $r_0 = 0$ and $r_H = 3.5074\sqrt{\mu}$ ($\mu > 0$). The r_0 is the equilibrium solution E_2, while the r_H represents the amplitudes of a family of limit cycles (periodic solutions). Their stability can be easily obtained from the first equation of (36) as follows:

$$r_0 : \begin{cases} \text{Stable} & \text{for} \quad \mu < 0, \\ \text{Unstable} & \text{for} \quad \mu > 0 \end{cases}$$
$$r_H : \text{Stable} \quad \text{for} \quad \mu > 0.$$

r_H is stable because the coefficient of the third-order term of the first equation of (36) is negative, indicating that the Hopf bifurcation is supercritical, and the bifurcating limit cycles are asymptotically stable. The solution r_H can be used to estimate the amplitude of the limit cycles when a value of μ is given, while the second equation of (36) can be used to estimate the frequency of the bifurcating periodic solutions, which is given by $\dot{\theta} = 0$, resulting in

$$\omega = 0.3919579290 + 0.0222930658\mu - 0.0042326886r_H^2 = 0.3919579290 - 0.0297767861\mu. \tag{37}$$

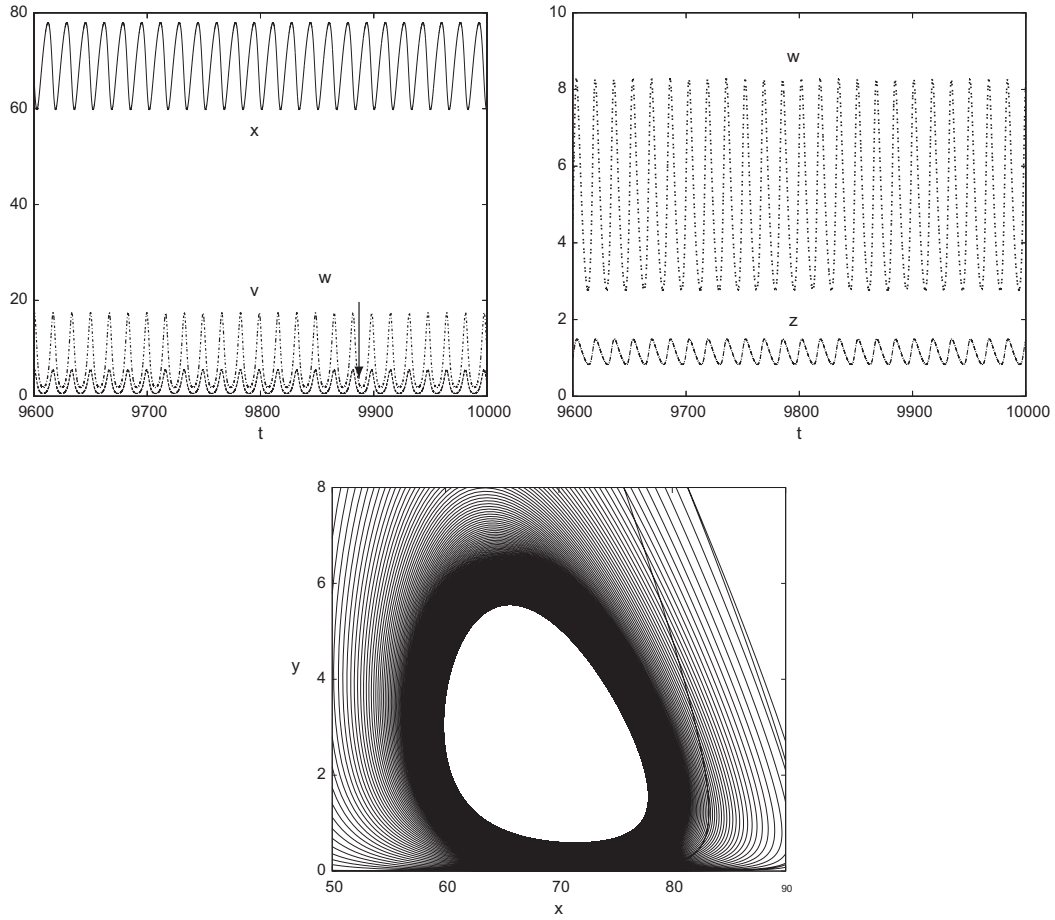

Fig. 4. Simulation of system (4) for the parameters given in (32) and $\lambda = 10.5$, showing stable periodic solutions in time history and a stable limit cycle in phase portrait, projected on the x–y place.

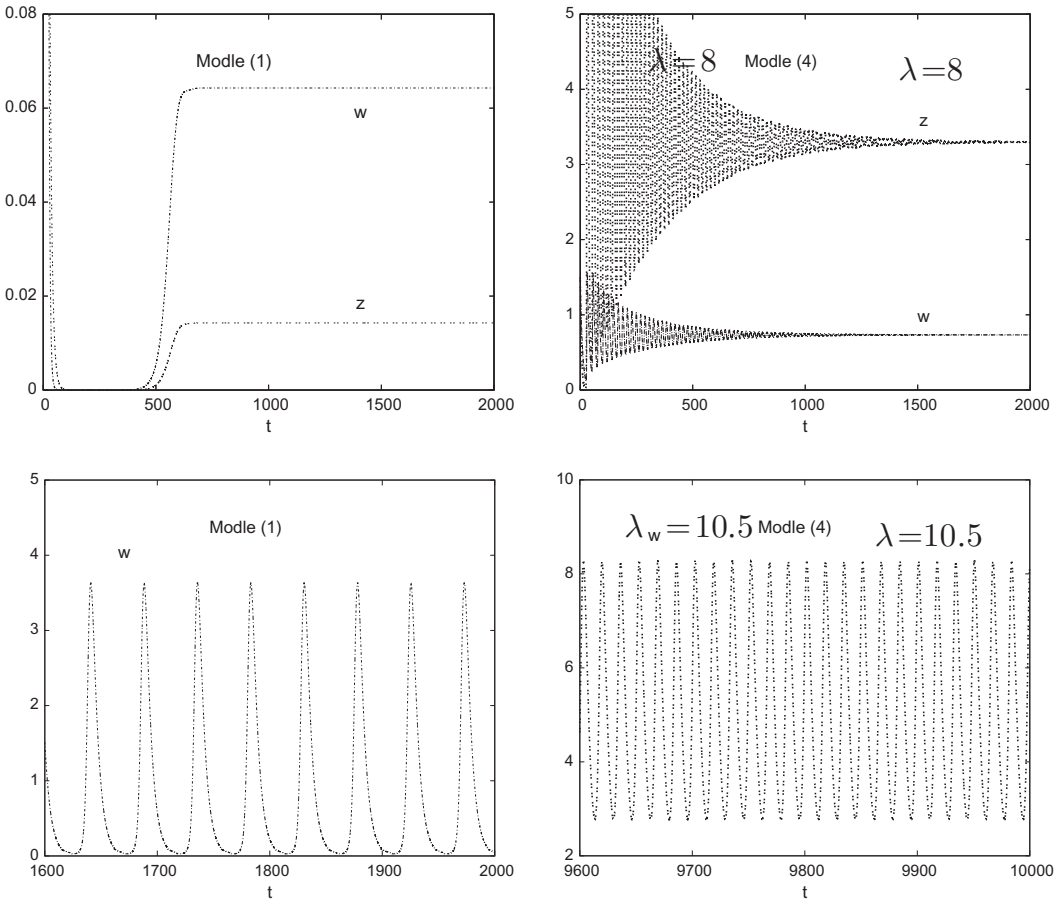

Fig. 5. Comparison between model (1) and model (4) with $\lambda = 8$ and $\lambda = 10.5$.

For simulation, we take $\lambda = 10.5$ (i.e., $\mu = 0.4138908734$). The simulation result is shown in Fig. 4, indicating that a stable limit cycle is obtained, as expected. But it is noted that the convergence of all the state variables is very slow, taking much longer time (almost 5 times than that for the case $\lambda = 8$, shown in Fig. 3)) to reach the stable limit cycle. For the value of $\mu = 0.4138908734$, we obtain the approximation $r_H \approx 2.2465$. We should not directly use this approximation to compare it with the amplitude of the limit cycle depicted in the phase portrait in Fig. 4, since we need to use the nonlinear transformation (which is available from the Maple output) and then the linear transformation T to make an accurate comparison. We omit the details here for brevity. However, we can easily check the frequency of the limit cycle. For $\mu = 0.4138908734$, $\omega \approx 0.37963359$, which yields the period $\frac{2\pi}{\omega} \approx 16.55$ (days). On the other hand, it can be observed from Fig. 4 that about 24 oscillations occur in the interval $t \in [9600, 10000]$ and so the period approximately equals $\frac{10000-9600}{24} \approx 16.67$ (days), which gives only 0.7% error compared to the theoretical prediction.

6. Discussion and conclusion

In this paper, we have studied a more realistic 5-dimensional in-host model which shows rich dynamic behaviors, in particular, on stability and bifurcations. The interaction between the uninfected cells, infected cells, virus, CTL response and CTL effector leads to a series of bifurcations through three equilibrium solutions: the infection-free equilibrium, E_0, the infectious equilibrium without CTL, E_1, and the infectious equilibrium with CTL, E_2. When the basic reproduction number, $R_0 \in (0, 1)$, the E_0 is globally asymptotically stable; when $R_0 \in (1, R_1)$, the E_1 is globally asymptotically stable; while for $R_0 \in (R_1, R_H)$, the E_2 is asymptotically stable. The E_0 and E_1 exchange their stability at the transcritical point $R_0 = 1$; and the E_1 and E_2 exchange their stability at the transcritical point $R_0 = R_1$; while the E_2 may lose its stability at a Hopf critical point $R_0 = R_H$, from which a family of limit cycles bifurcates. When the parameters are varying, as R_0 increases to cross the critical values 1 and R_1, the transcritical bifurcations can always occur from E_0 and E_1. However, whether the Hopf bifurcation from E_2 happens depends upon the parameter values. It may have no Hopf bifurcation, or two Hopf bifurcations. For example, as shown in Section 5.4, for the chosen parameter values (in particular for $u = 8$), there exist two Hopf critical points R_{H_1} and R_{H_2}, and the equilibrium

E_2 is asymptotically stable for $R_0 \in (R_1, R_{H_1}) \bigcup (R_{H_2}, \infty)$. But if we decrease u from $u = 8$, we find that two Hopf critical points merges into one, and then the Hopf bifurcation disappears. The critical value of u at which the two Hopf critical points merges is $u_c = 7.0631749350\cdots$ for which $\lambda_H = 19.8867998387\cdots$. Thus, there is no Hopf bifurcation for $u < u_c$ and two Hopf bifurcations for $u > u_c$ from the equilibrium E_2. Certainly, we may change other parameters to obtain various sets of parameter values such that either no Hopf bifurcation or two Hopf bifurcations occur from the equilibrium E_2.

The qualitative analysis gives a clear big picture for the dynamical behavior of the model. Moreover, one can perform parametric studies to provide information for controlling the disease. With the theoretical predictions as guidelines, we can further use numerical simulation to consider transient dynamical behavior of the model for different values of parameters. For example, comparing the results shown in Figs. 1–3 indicates that when the parameter λ is increasing, the transient behavior of the model can be monotonic (for $\lambda = 1.5$ which shows convergence to E_0, see Fig. 1), monotonic with some "overshooting" (for $\lambda = 2.5$ which shows convergence to E_1, see Fig. 2), or purely oscillating (for $\lambda = 8$ which shows convergence to E_2, see Fig. 3). Further, it is seen from these figures that the larger the λ is taken, the slower the convergence speed becomes.

Finally, we would like to make a remark on the comparison of the results given in [9] for model (1) and that presented in this paper, showing some interesting observations, since the same parameter values given in (32) (except k and u used in this paper) are used in the simulations. The results shown in Fig. 1 with $\lambda = 1.5$ have a similar trend in a very close time frame to that shown in Fig. 1 in [9], where though $\lambda = 3$ is used. Comparing the results in Fig. 2 with $\lambda = 2.5$ to that in Fig. 2 in [9] with $\lambda = 7.5$ again shows a similar trend, but the convergence time to reach the final steady-state values are different that our 5-dimensional model (4) takes almost double time of that taken by the 4-dimensional model (1). This is perhaps due to the model (1) lacking the virus equation and different values of λ used. More interesting phenomena can be observed from Figs. 3 and 4. In order to make a consistent comparison, we put the simulation results for model (1) and model(4) together in Fig. 5 for $\lambda = 8$ and $\lambda = 10.5$, showing the CTL property. It can be seen from Fig. 5 that for $\lambda = 8$, the equilibrium E_2 is stable, and the 4-dimensional model (1) shows a similar convergence trend as that in previous cases except a very short oscillating at the beginning, while the new model (4) shows a continuous oscillating behavior till reaching the equilibrium E_2. Moreover, the new model shows a slower convergent speed, almost taking 3 times of that for model (1) to reach the equilibrium. The last comparison for $\lambda = 10.5$, for which periodic solutions bifurcate from a Hopf critical point. For this case, the dynamical behaviors are similar, but our new model takes longer time (almost five times of that for model (1)) to get its steady-state value. Moreover, it is noted that the ratio of the periods of the periodical solutions for model (1) to model (4) is approximately equal to $(400/8.4)/(400/24) \approx 2.857142857$. These observations of difference between our 5-dimensional model (4) and the 4-dimensional model (1) [9] imply that the virus is necessary to be involved in the modeling. This suggests that quasi-steady state assumption should be applied carefully, which may miss some important dynamical behavior of the system.

Acknowledgment

This work was supported by the Natural Science and Engineering Research Council of Canada (NSERC, No. R2686A02), and the National Natural Science Foundation of China (NNSFC, No. 11201294) and the Innovation Program of Shanghai Municipal Education Commission (No. 14YZ114).

References

[1] Adams BM, Banks HT, Davidian M, Kwon HD, Tran HT, Wynne SN, et al. HIV dynamics: modeling, data analysis, and optimal treatment protocols. J Comput Appl Math 2005;184(1):10–49.
[2] Rong L, Perelson AS. Modeling HIV persistence, the latent reservoir, and viral blips. J Theor Biol 2009;260(2):308–31.
[3] Rong L, Perelson AS. Modeling latently infected cell activation: viral and latent reservoir persistence, and viral blips in HIV-infected patients on potent therapy. PLoS Comput Biol 2009;5(10):e1000533.
[4] Hernandez-Vargas EA, Middleton RH. Modelling the three stages in HIV infection. J Theor Biol 2013;320:33–40.
[5] Zhang W, Wahl L, Yu P. Conditions for transient viremia in deterministic in-host models: viral blips need no exogenous trigger. SIAM J Appl Math 2013;73(2):853–81.
[6] Callaway DS, Perelson AS. HIV-1 infection and low steady state viral loads. Bull Math Biol 2002;64(1):29–64.
[7] Perelson AS, Kirschner DE, De Boer R. Dynamics of HIV infection of $CD4^+$ T cells. Math Biosci 1993;114(1):81–125.
[8] Finzi D, Blankson J, Siliciano JD, Margolick JB, Chadwick K, Pierson T, et al. Latent infection of CD4+ T cells provides a mechanism for lifelong persistence of HIV-1, even in patients on effective combination therapy. Nat Med 1999;5(5):512–7.
[9] Chan BS, Yu P. Bifurcation analysis in a model of cytotoxic T-lymphocyte response to viral infections. Nonlinear Anal Real World Appl 2012;13(1):64–77.
[10] Terai C, Kornbluth RS, Pauza CD, Richman DD, Carson DA. Apoptosis as a mechanism of cell death in cultured T lymphoblasts acutely infected with HIV-1. J Clin Invest 1991;87(5):1710.
[11] Perelson AS, Neumann AU, Markowitz M, Leonard JM, Ho DD. HIV-1 dynamics in vivo: virion clearance rate, infected cell life-span, and viral generation time. Science 1996;271(5255):1582–6.
[12] Schnittman SM, Greenhouse JJ, Psallidopoulos MC, Baseler M, Salzman NP, Fauci AS, et al. Increasing viral burden in CD4+ T cells from patients with human immunodeficiency virus (HIV) infection reflects rapidly progressive immunosuppression and clinical disease. Ann Internal Med 1990;113(6):438–43.
[13] Nowak MA, Bangham CR. Population dynamics of immune responses to persistent viruses. Science 1996;272(5258):74–9.
[14] Wodarz D, Page KM, Arnaout RA, Thomsen AR, Lifson JD, Nowak MA. A new theory of cytotoxic T-lymphocyte memory: implications for HIV treatment. Philos Trans R Soc London Ser B 2000;355(1395):329–43.
[15] De Boer R, Perelson A. Target cell limited and immune control models of HIV infection: a comparison. J Theor Biol 1998;190(3):201214.
[16] Anderson R, May R. Infectious diseases of humans: dynamics and control. Oxford University Press; 1991.
[17] Wodarz D, Nowak MA. Mathematical models of HIV pathogenesis and treatment. BioEssays 2002;24(12):1178–87.

[18] Wodarz D, Nowak MA. Specific therapy regimes could lead to long-term control of HIV. Proc Natl Acad Sci USA 1999;96:14464–9.
[19] Jiang X, Yu P, Yuan Z, Zou X. Dynamics of an HIV-1 therapy model of fighting a virus with another virus. J Biol Dyn 2009;3(4):387–409.
[20] Revilla T, Garca-Ramos G. Fighting a virus with a virus: a dynamic model for HIV-1 therapy. Math Biosci 2003;185(2):191–203.
[21] Yu P, Zou X. Bifurcation analysis on an HIV-1 model with constant injection of recombinant. Int J Bifurcation Chaos 2012;22(3):1250062 (p. 21).
[22] Smith HL. Monotone dynamical systems: an introduction to the theory of competitive and cooperative systems. Mathematical Surveys and Monographs, vol. 41. Providence, RI: American Mathematical Society; 1995.
[23] Yu P. Closed-form conditions of bifurcation points for general differential equations. Int J Bifurcation Chaos 2005;15(4):1467–83.
[24] Hinrichsen D, Pritchard AJ. Mathematical systems theory I: modelling, state space analysis, stability and robustness. Texts in Applied Mathematics, vol. 48. Springer; 2005.
[25] Hirsch WM, Herman H, Gabriel JP. Differential equation models of some parasitic infections: methods for the study of asymptotic behavior. Commun Pure Appl Math 1985;38(6):733–53.
[26] Korobeinikov A. Global properties of basic virus dynamics models. Bull Math Biol 2004;66(4):879–83.
[27] Yu P. Computation of normal forms via a perturbation technique. J Sound Vib 1998;211(1):19–38.
[28] Yu P, Huseyin K. A perturbation analysis of interactive static and dynamic bifurcations. IEEE Trans Autom Control 1988;33(1):28–41.